A metamaterial absorber with direction-selective and polarisation-insensitive properties*

Gu Chao(顾 超)[a], Qu Shao-Bo(屈绍波)[a)b)†], Pei Zhi-Bin(裴志斌)[a], and Xu Zhuo(徐 卓)[b]

[a] *The College of Science, Air Force Engineering University, Xi'an* 710051, *China*
[b] *Electronic Materials Research Laboratory, Key Laboratory of Ministry of Education, Xi'an Jiaotong University, Xi'an* 710049, *China*

(Received 10 May 2010; revised manuscript received 12 July 2010)

This paper reports the design of a metamaterial absorber with direction-selective and polarisation-insensitive property. Both theoretical and simulated results reveal that the absorber has a distinct absorption point with direction selectivity at 7.48 GHz, which is related to the resonance of the metamaterial and is not influenced by the polarisation. The retrieved impedance indicates that the impedance of the absorber can be tuned to approximatively match the impedance of the free space on one side and not to match the impedance of the free space on the other side. This design can result in the minimal reflectance, the minimal transmission and the highest absorbance at the absorption frequency. The distribution of the power loss indicates that the absorber is an excellent electromagnetic wave collector: the wave is first trapped and reinforced in certain specific locations, and then mostly consumed. The distribution of the surface current is consistent with the design, the retrieved impedance and the distribution of the power loss. This absorber may have applications in many scientific and technological areas.

Keywords: metamaterial absorber, direction-selective, polarisation-insensitive

PACS: 78.20.Ci, 41.20.Jb **DOI:** 10.1088/1674-1056/20/3/037801

1. Introduction

Electromagnetic metamaterial (MM) has produced exotic effects such as the negative index of refraction,[1,2] and interesting devices such as an electromagnetic cloak device.[3] The realization of such properties lies in the ability of MM to independently tailor the electric[4] and the magnetic[5] responses to incident radiation. The MM is also geometrically scalable, which translates into operability over a large portion of the electromagnetic spectrum. So far, the MM has been demonstrated in every technologically relevant spectral range, from radio,[6] microwave,[7,8] mm-Wave,[9] THz,[10] mid-infrared (MIR),[11] near-infrared (NIR),[12] to the near optical.[13] The MM is an ideal material for the investigation of novel physical phenomena and also holding great promise for future applications.

Recently, the design of resonant metamaterial absorber (MA) at microwave and terahertz bands has attracted much attentions.[14−17] By adjusting the dimensions of the MM, a "perfect" absorber with near-unity absorbance can be realized in the GHz regime.[14] In the terahertz regime, several absorbers have been demonstrated.[15−17] All these absorbers are composed of an electric split-ring resonator (eSRR) layer and a metal wire or plate layer, which decides the polarisation-sensitive property of these absorbers. However, absorbers with polarisation-insensitive property are desirable, but still lacking. In this work, we propose an MA having a distinct absorption point at 7.48 GHz. The special feature of our MA is that our structure exhibits direction selectivity and polarisation insensitivity. Both theoretical and simulated results reveal that our MA has a direction-selective absorption point at 7.48 GHz, which is related to the resonance of the metamaterial and is not influenced by the polarisation.

2. Design and simulation

A unit cell of our MA consisted of two square metallic rings and a substrate is shown in Fig. 1. The electric coupling was supplied by the coupling of the square metallic rings in the same plane. The magnetic

*Project supported by the National Natural Science Foundation of China (Grant Nos. 50632030, 60871027, 60901029 and 61071058), in part by the 973 Project of Science and Technology Ministry of China (Grant No. 2009CB623306) and the Shaanxi Provincial Synthetic Electronic Information System Foundation, China (Grant No. 200905A).
†Corresponding author. E-mail: qushaobo@mail.xjtu.edu.cn
© 2011 Chinese Physical Society and IOP Publishing Ltd

coupling was supplied by the coupling of the square metallic rings between parallel planes separated by the substrate as shown in Fig. 1(c). This frame is similar to short wire pairs in Ref. [11], in that Linden *et al.* derived a magnetic response from driving two antiparallel currents in conducting segments. We were then able to tune the electromagnetic response by changing the geometries of the small ring and the big ring, and the separation between them. To maximize the absorption of the device, we should minimize both transmission and reflection. So the impedance of our absorber should be tuned to approximatively match the impedance of the free space on one side and not to match the impedance of the free space on the other side. This design could result in the minimal reflectance, the minimal transmission and the highest absorbance at the absorption frequency.

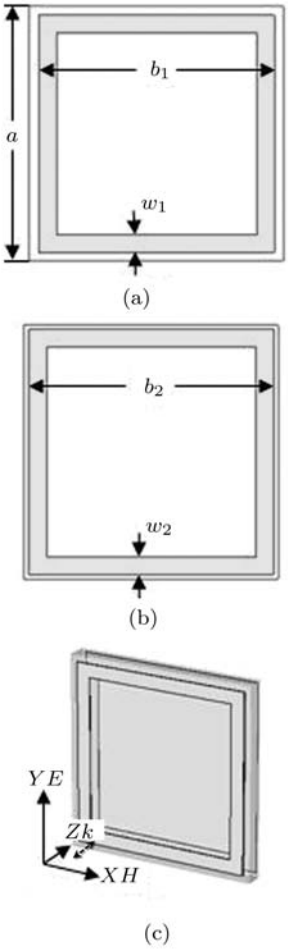


Fig. 1. The small ring (a) and the big ring (b). Dimension notations are listed in (a) and (b). The unit cell is shown in (c) with an arrow indicating the propagation direction.

We performed computer simulations of the MA using the commercial finite difference time domain solver (CST Microwave Studio 2008). The programme simulated a single unit cell as shown in Fig. 1(c) with proper boundary conditions, i.e., perfect electric boundary (XZ-plane) and perfect magnetic boundary (YZ-plane). Waveguide ports on the other boundaries ($-Z$ is port 1, $+Z$ is port 2) simulated a transverse electromagnetic (TEM) plane wave propagating through the medium. Utilizing CST, we optimise the structure of the MA and list the obtained size parameters in Figs. 1(a) and 1(b), $b_1 = 5.3$, $w_1 = 0.4$, $b_2 = 5.5$, $w_2 = 0.4$, $a = 5.7$ mm. The substrate is 0.6 mm thick ($\varepsilon_r = 4.9$, $t_d = 0.025$) and the copper film is 0.017 mm thick. The simulation produced the complex frequency dependent S parameters, S_{11}, S_{21}, S_{22} and S_{12}. Then, we could calculate the frequency dependent absorbances by $A_1(\omega) = 1 - |S_{11}|^2 - |S_{21}|^2$, $A_2(\omega) = 1 - |S_{22}|^2 - |S_{12}|^2$. The result is shown in Fig. 2. From Fig. 2, when the wave propagates along $+Z$, there is a distinct absorption peak located at 7.48 GHz, with absorbance 99.1%. The absorption bandwidth, defined as full width at half maximum, is 330 MHz for the absorption peak. However, when the wave propagates along $-Z$, there is undistinguishable absorption located at 7.48 GHz, with absorbance 1.6%. These results indicate that our MA has a strong direction selectivity.

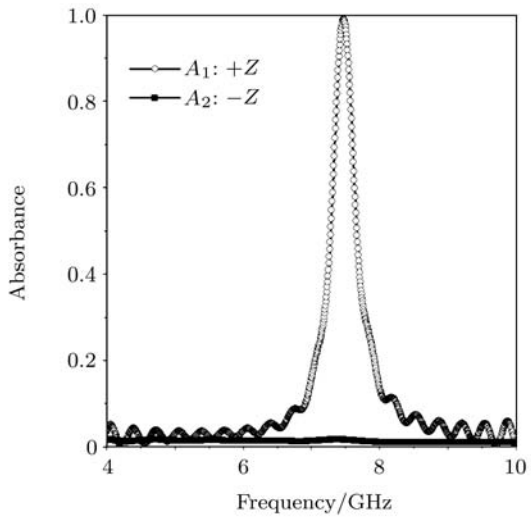


Fig. 2. The simulated MA's absorbances for two different transmission directions.

On the other hand, the configuration in Fig. 1(c) is polarisation-insensitive. Evidence can be seen in Fig. 3, where we plot the simulated absorbances versus different polarisation angles for transmissions of both directions. As shown in Fig. 3(a), when the wave propagates along $+Z$, the absorbances for different polarisation angles are the same. At 7.48 GHz, all absorbances are 99.1%. From Fig. 3(b), when the wave

propagates along $-Z$, the absorbances for different polarisation angles are also approximatively the same. At 7.48 GHz, all absorbances are 1.6%. These results indicate that the MA is polarisation-insensitive.

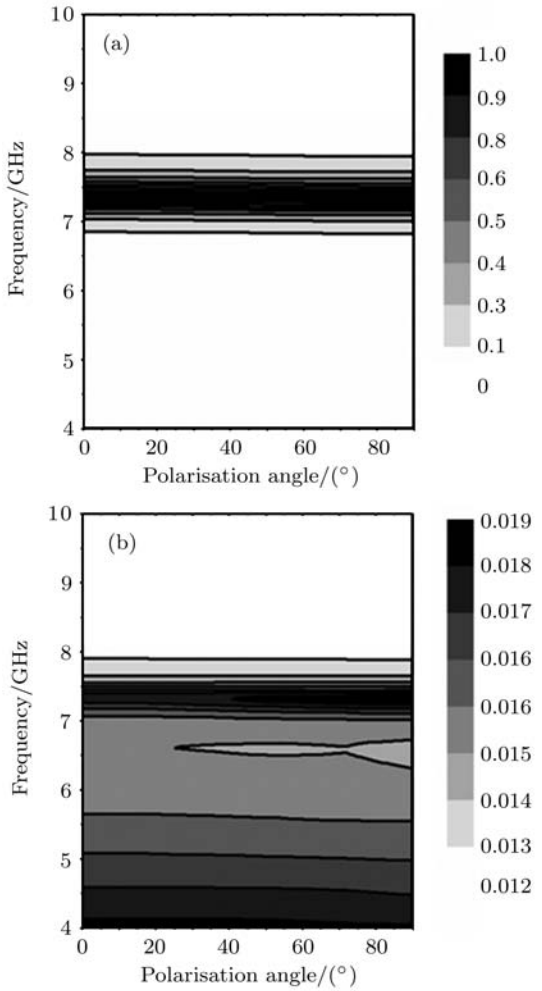


Fig. 3. The simulated absorbances versus different polarisation angles for transmissions of different directions: (a) the wave propagates along $+Z$; (b) the wave propagates along $-Z$.

Then we can retrieve the complex wave impedance from the simulated S parameters for the two different transmission directions. The results are shown in Fig. 4. When the wave propagates along $+Z$, the real part of the retrieved impedance is 1.16 at 7.48 GHz, which is consistent with our intent to match the impedance of the free space on one side. When the wave propagates along $-Z$, the real part of the retrieved impedance is 0.03 at 7.48 GHz, which does not match the impedance of the free space. These results indicate that the impedance of our MA can be tuned to approximatively match the impedance of the free space on one side and not to match the impedance of the free space on the other side at the absorption frequency. This design can result in the minimal reflectance, the minimal transmission and the highest absorbance at the absorption frequency.

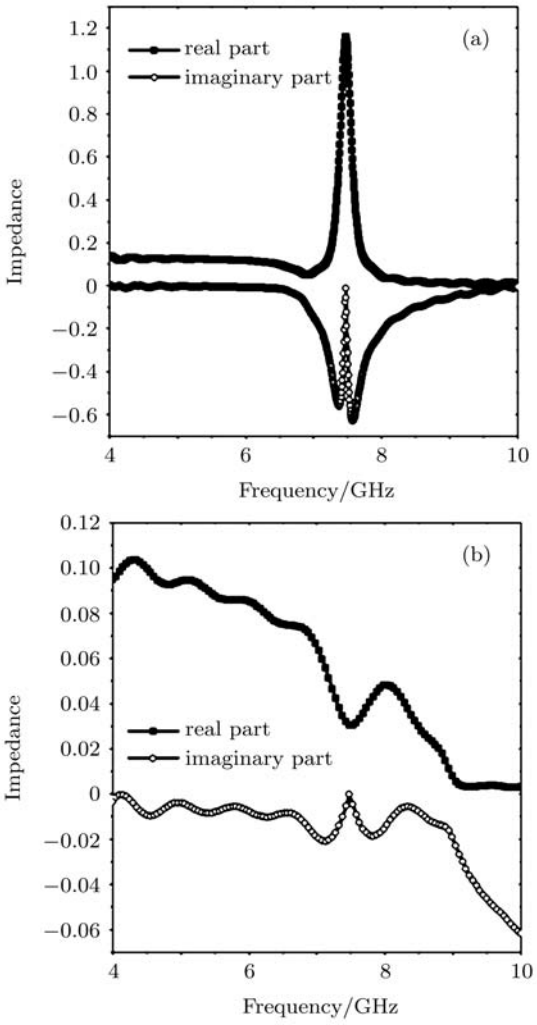


Fig. 4. The retrieved impedance: (a) the wave propagates along $+Z$; (b) the wave propagates along $-Z$.

3. The power loss and the surface current

It is also interesting to explore the power loss in the MA since it can provide information about how and where the absorption happens. The distribution of the power loss in the MA at 7.48 GHz was calculated and compared for the two different transmission directions. Figures 5(a) and 5(c) show the normal views of the power loss. The side views of the power loss, as plotted in Figs. 5(b) and 5(d), provide detailed information about the absorption occurred in different layers. As shown in Figs. 5(a) and 5(b) (the wave propagating along $+Z$), most power loss occurs at space between the rings (the top and bottom lo-

cations in the Y direction), which indicates that the major component responsible for $A_1(\omega)$ is dielectric loss of the substrate. These results indicate that the MA can concentrate the electromagnetic wave in some specified locations, where the energy is reinforced and subsequently converted into thermal energy, leading to a strong absorption. In Figs. 5(c) and 5(d) (the wave propagating along $-Z$), we know that there is no distinct power loss in the MA, which once again indicates that our MA has a strong direction selectivity.

The distribution of the surface current in the MA was also calculated and compared for the two different transmission directions. In Fig. 6, we present a vector plot of the surface current density in the MA at 7.48 GHz for the two different transmission directions. In Figs. 6(a) and 6(b) (the wave propagates along $+Z$), we observe antiparallel currents on the small ring and the big ring, which are driven by the resonance of the metamaterial. In Figs. 6(c) and 6(d) (the wave propagates along $-Z$), the currents in the MA are weak, which indicates that the resonance of metamaterial is quite weak. These results are consistent with our design, the retrieved impedance and the distribution of the power loss.

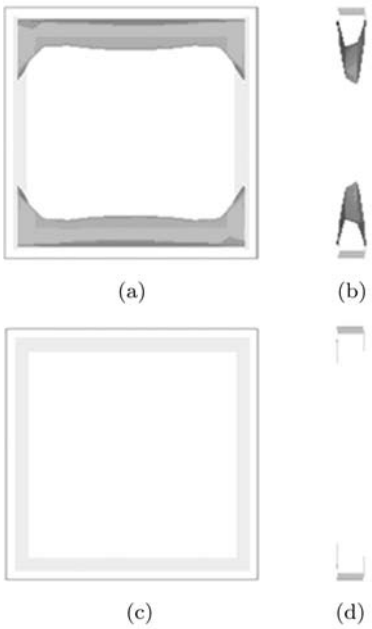


Fig. 5. The distribution of the power loss in the MA at 7.48 GHz. The normal views: (a) the wave propagates along $+Z$; (c) the wave propagates along $-Z$. The side views: (b) the wave propagates along $+Z$; (d) the wave propagates along $-Z$.

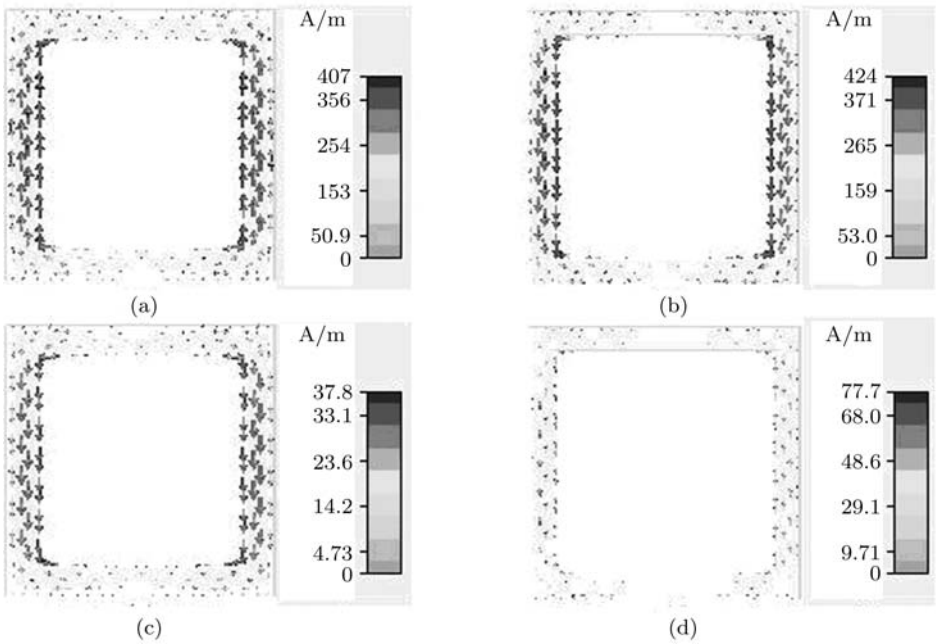


Fig. 6. The distribution of the surface current density in the MA at 7.48 GHz for the two different transmission directions: (a) and (b) the wave propagates along $+Z$; (c) and (d) the wave propagates along $-Z$.

4. Conclusion

In summary, we present a metamaterial absorber with direction-selective and polarisation-insensitive property. The retrieved impedance indicates that the impedance of our absorber can be tuned to approximatively match the impedance of the free space on one side and not to match the impedance of the free

space on the other side. This design can result in the minimal reflectance, the minimal transmission and the highest absorbance at the absorption frequency. The simulated absorbances for different polarisation angles for two different transmission directions validate the polarisation-insensitive property of the MA. The absorption mechanism was theoretically investigated by simulating the power loss in the MA, which shows that the MA is an excellent electromagnetic wave collector, which traps the electromagnetic wave into some specific locations of the devices and then strongly absorbs it. The distribution of the surface current is consistent with our design, the retrieved impedance and the distribution of the power loss.

The design presented here is geometrically scalable. Therefore, our results are not limited to GHz frequencies and may be used in other portions of the electromagnetic spectrum, such as the THz frequencies.

References

[1] Veselago V G 1968 *Sov. Phys. Usp.* **10** 509

[2] Shelby R A, Smith D R and Schultz S 2001 *Science* **292** 77

[3] Schurig D, Mock J J, Justice B J, Cummer S A, Pendry J B, Starr A F and Smith D R 2006 *Science* **314** 977

[4] Pendry J B, Holden A J, Stewart W J and Youngs I 1996 *Phys. Rev. Lett.* **76** 4773

[5] Pendry J B, Holden A J, Robbins D J and Stewart WJ 1999 *IEEE Trans. Microwave Theory Tech.* **47** 2075

[6] Wiltshire M C K, Pendry J B, Young I R, Larkman D J, Gilderdale D J and Hajnal J V 2001 *Science* **291** 849

[7] Luo C R, Wang S H, Guo J Q, Huang Y and Zhao X P 2009 *Acta Phys. Sin.* **58** 3124 (in Chinese)

[8] Zhang S, Qu S B, Ma H, Xie F and Xu Z 2009 *Acta Phys. Sin.* **58** 3961 (in Chinese)

[9] Gokkavas M, Guven K, Bulu I, Aydin K, Penciu R S, Kafesaki M, Soukoulis C M and Ozbay E 2006 *Phys. Rev.* B **73** 193103

[10] Yen T J, Padilla W J, Fang N, Vier D C, Smith D R, Pendry J B, Basov D N and Zhang X 2004 *Science* **303** 1494

[11] Linden S, Enkrich C, Wegener M, Zhou J F, Koschny T and Soukoulis C M 2004 *Science* **306** 1351

[12] Zhang S, Fan W, Panoiu N C, Malloy K J, Osgood R M and Brueck S R J 2005 *Phys. Rev. Lett.* **95** 137404

[13] Tang S W, Zhu W R and Zhao X P 2009 *Acta Phys. Sin.* **58** 3220 (in Chinese)

[14] Landy N I, Sajuyigbe S, Mock J J, Smith D R and Padilla W J 2008 *Phys. Rev. Lett.* **100** 207402

[15] Tao H, Landy N I, Bingham C M, Zhang X, Averitt R D and Padilla W J 2008 *Opt. Express* **16** 7181

[16] Tao H, Bingham C M, Strikwerda A C, Pilon D, Shrekenhamer D, Landy N I, Fan K, Zhang X, Padilla W J and Averitt R D 2008 *Phys. Rev.* B **78** 241103(R)

[17] Landy N I, Bingham C M, Tyler T, Jokerst N, Smith D R and Padilla W J 2009 *Phys. Rev.* B **79** 125104